Connectivity Analysis of Cognitive Radio Ad-hoc Networks with Shadow Fading

Le The Dung[1] and Beongku An[2]
[1] Dept. of Electronic & Computer Engineering in Graduate School, Hongik University
Republic of Korea
[e-mail: thedung_hcmut@yahoo.com]
[2] Dept. of Computer & Information Communications Engineering, Hongik University
Republic of Korea
[e-mail: beongku@hongik.ac.kr]
*Corresponding author: Beongku An

Received April 10, 2015; revised June 27, 2015; accepted July 22, 2015; published September 30, 2015

Abstract

In this paper, we analyze the connectivity of cognitive radio ad-hoc networks in a log-normal shadow fading environment. Considering secondary user and primary user's locations and primary user's active state are randomly distributed according to a homogeneous Poisson process and taking into account the spectrum sensing efficiency of secondary user, we derive mathematical models to investigate the connectivity of cognitive radio ad-hoc networks in three aspects and compare with the connectivity of ad-hoc networks. First, from the viewpoint of a secondary user, we study the communication probability of that secondary user. Second, we examine the possibility that two secondary users can establish a direct communication link between them. Finally, we extend to the case of finding the probability that two arbitrary secondary users can communicate via multi-hop path. We verify the correctness of our analytical approach by comparing with simulations. The numerical results show that in cognitive radio ad-hoc networks, high fading variance helps to remarkably improve connectivity behavior in the same condition of secondary user's density and primary user's average active rate. Furthermore, the impact of shadowing on wireless connection probability dominates that of primary user's average active rate. Finally, the spectrum sensing efficiency of secondary user significantly impacts the connectivity features. The analysis in this paper provides an efficient way for system designers to characterize and optimize the connectivity of cognitive radio ad-hoc networks in practical wireless environment.

Keywords: Ad-hoc wireless networks, cognitive radio ad-hoc networks, shadow fading, node's communication probability, direct communication link probability, multi-hop connectivity

This work was supported by the National Research Foundation of Korea (NRF) grant funded by the Korea government (MSIP) (No. 2012R1A2A2A01046780).

http://dx.doi.org/10.3837/tiis.2015.09.004 **ISSN : 1976-7277**

1. Introduction

Nowadays, technological advances together with the demands for efficient and flexible networks have led to the development of wireless ad-hoc networks where wireless devices can communicate with each other in a peer-to-peer fashion without relying on any fixed infrastructure. With the fast increase in the number of wireless devices, the industrial, scientific, and medical (ISM) bands are getting congested. Meanwhile, many other licensed spectrum bands are allocated through static polices. Studies sponsored by the Federal Communication Commission (FCC) observe that the average utilization of such bands varies between 15% and 18% [1]. To alleviate such inefficient spectrum resource utilization, a promising technology named cognitive radio is proposed. Cognitive radio technology enables unlicensed users to opportunistically utilize the licensed spectrum band in a dynamic and non-instructive manner so that they do not interfere with the operation of licensed users. In this framework, Cognitive Radio Ad-Hoc Networks (CRAHNs) [2] are formed by cognitive radio nodes that communicate in distributed fashion by sharing licensed spectrum bands. In these networks, there are two kinds of users: Primary Users and Secondary Users. Primary Users (PUs) have the right to use licensed spectrum while Secondary Users (SUs) have to sense and detect available spectrum opportunities to be used for transmission. Every SU can opportunistically access a licensed spectrum band not used by a PU and it has to immediately vacate this spectrum band when the PU becomes active.

To model network level properties of CRAHNs, stochastic geometry [3] and percolation theory [4] are often used. In other words, percolation theory is targeted at random geographic graph where the nodes are random distributed and node's transmission range is assumed to be a disk (i.e. a circle). This assumption is applied in designing routing protocols [5-6] as well as analyzing connectivity of CRAHNs.

So far, percolation-based connectivity has been investigated in distributed networks such as ad-hoc and wireless sensor networks [7-8]. Recently, the connectivity of CRAHNs has also been studied from the perspective of stochastic geometry and percolation theory. In [9], the concept of *cognitive algebraic connectivity*, i.e., the second smallest eigenvalue of the Laplacian of a cognitive network graph is introduced. Then, this notion is used as metric for routing design in CRAHNs. The authors in [10] define *connectivity region* as the set of density pair – the density of SUs, λ_{SU}, and the density of PUs, λ_{PT}, under which the secondary network is connected. By using theories and techniques from continuum percolation, they derive the relation between the connectivity of a secondary network and the pair (λ_{SU}, λ_{PT}). In [11], the authors introduce the *cognitive radio graph model* (CRGM) that takes into account the impact of the number of channels and the activities of PUs, and then combine the CRGM with continuum percolation model to study the connectivity of secondary network. On the basic of random geometric graph and probability theory, in [12], a method that divides connectivity of CRAHNs into topological connectivity and physical connectivity is proposed to derive a close-form formula of connectivity between two SUs. In [13], taking correct detection and false alarm probabilities (P_d and P_f), the authors derive a close-form model for the critical thinned density λ_S^* of active SUs in a secondary network, that is, the density of SUs at which full connectivity of secondary network is ensured. Moreover, the percolation of the secondary network is investigated by using percolation confidence defined as the ratio of number SUs connected with the main component to the number of all active SUs in the secondary network.

Although a more accurate modeling of physical layer is indeed important in network-level research on CRAHNs, all of aforementioned papers study the connectivity-related properties

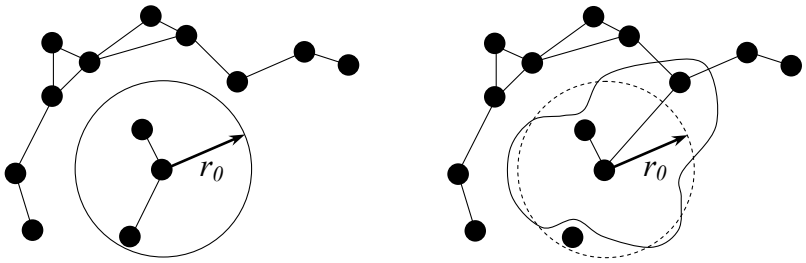

(a) Disk link model (b) Shadow fading link model

Fig. 1. Illustration of link models and resulting connectivity

by using a ideal disk link model to characterize the wireless channel, i.e. two nodes are connected if and only if the relative distance between them is less or equal to a certain threshold distance r_0, called transmission range as in **Fig. 1(a)**. Such disk link model only reflects deterministic, distance-dependent wireless channel. However, the wireless channel can be modeled in a more practical manner as in **Fig. 1(b)**. Particularly, the randomness of channel condition induced by shadowing effects that are caused by obstacles in the networks should be taken into consideration.

In the literature, studies on the impact of different types of fading such as log-normal shadow fading, Rayleigh fading, and Nakagami-*m* fading on the connectivity of ad-hoc networks are presented in [14-16], respectively. Recently, investigation on the connectivity of CRAHNs with fading has attracted much research attention [17, 18]. Particularly, the authors in [17] investigate the local connectivity, i.e. node degree and probability of node isolation of CRAHNs by using stochastic geometry [3] and probability theory. However, the influence of spectrum sensing efficiency of SU on local network connectivity is not considered and no results on link connectivity and multi-hop path connectivity are presented. In [18], using percolation theory [4], the authors derive the closed-form expression of the outage probability of PU due to inter-network interference (SU to PU) with the sensing error of SU is taken into account and the upper and lower bounds of percolation area within which the secondary network percolates. Thus, this work aims at dense networks.

The aforementioned observations motivate us to derive mathematical models in a simple intuitive approach for analyzing the connectivity of CRAHNs with shadow fading. Taking into

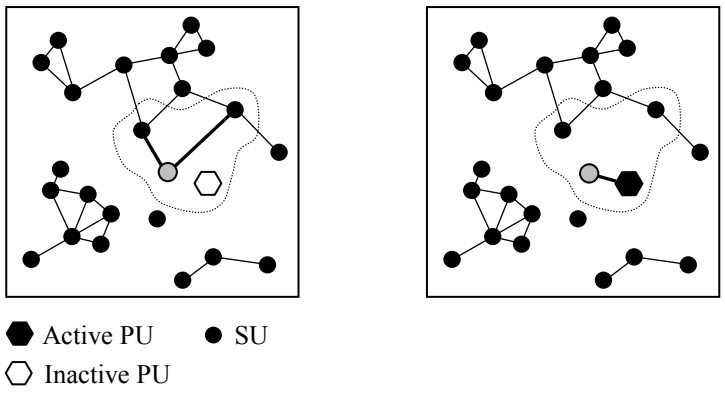

Fig. 2. The impact of shadow fading and PU existence on the connectivity of CRAHNs

account the spatial-temporal spectrum availability and spectrum sensing efficiency of SU, our mathematical models can be used to analyze three important connectivity-related features of secondary networks, e.g. communication probability of SU, probability of direct communication between two SUs, and the multi-hop connectivity of two arbitrary SUs in the network area. In addition, the models can be applied for both sparse and dense networks. **Fig. 2** illustrates the influence of shadow fading and PU existence on the connectivity of CRAHNs. Obviously, with shadow fading wireless channel, node's transmission range is no longer a disk with radius r_0 as in previous researches. Instead, it becomes a stochastic variable, resulting in more complexity of connectivity analysis.

The rest of this paper is organized as follows. In Section 2, we introduce formally the system model used in this paper. In Section 3, we study the connectivity of CRAHNs in three aspects, e.g. communication probability of a SU, probability of direct communication between two SUs, and multi-hop connectivity of two arbitrary SUs in the network area. Section 4 presents numerical results of the influence of shadow fading and PU's existence on the connectivity in CRAHNs. Finally, Section 5 concludes this paper.

2. System model

2.1 Spatial node distribution

The distribution of nodes in this paper is given by a random process on a finite network area $a \times a$ with N nodes in total. Specifically, it can be approximately characterized by the homogeneous Poisson process of density $\rho = N / a^2$. This process has the following property:

– The number of nodes M in certain subarea A such as transmission area follows a Poisson distribution, i.e.,

$$P(m \text{ nodes in } A) = P_M(m) = \frac{\lambda^m}{m!} e^{-\lambda}, \tag{1}$$

where the expected value is $E[M] = \lambda = \rho A$. $E[M]$ can also be referred as the expected value of node degree $E[M]$, which will be discussed later.

2.2 Primary network

The primary network consists of primary transmitters and primary receivers distributed in network area according to homogeneous Poisson point process of density ρ_P [19], denoted by $G(\rho_P)$. The operation of primary transmitter on licensed spectrum band is associated with an independent and identical ON-OFF state where the number of times that primary transmitter occupy licensed spectrum in a time unit follows Poisson distribution with average active rate λ_P. Thus, the probability that there are x spectrum occupation events of active primary transmitter in a time unit is

$$P_X(x) = \frac{\lambda_P^x}{x!} e^{-\lambda_P} \tag{2}$$

where λ_p is the average active rate of primary user.

Each primary transmitter is associated with a primary receiver. Thus, the number of times that primary receiver is in active state in a time unit also follows Poisson distribution with average active rate λ_P.

2.3 Secondary network

The secondary network consists of N_S secondary users distributed in network area according to homogeneous Poisson point process of density ρ_S [19], denoted by $G(\rho_S)$. Without the impact of primary network, $G(\rho_S)$ models a standalone network as in AHNs. However, in temporal-spatial spectrum agility of CRAHNs as considered in this paper, the establishment of wireless communication link between two SUs depends on both channel quality and transmission opportunity. This issue will be mathematically studied in detail in Section 3.

2.4 Wireless channel model

To describe the wireless channel model used in this paper, we consider two nodes i and j locating at a relative distance $l(i, j)$. Node i transmits signal with power $p_t(i)$ and node j receives that signal with power $p_r(j)$. Thus, the signal attenuation between these two nodes is defined as

$$\gamma(i, j) = \frac{p_t(i)}{p_r(j)}, \tag{3}$$

and can be expressed in terms of dB as

$$\gamma(i, j) = 10\log_{10}\left(\frac{p_t(i)}{p_r(j)}\right) \text{ (dB)}. \tag{4}$$

In the shadow fading environment, $\gamma(i, j)$ consists of two components: a deterministic component $\gamma_1(i, j)$ and a stochastic component $\gamma_2(i, j)$. The deterministic component is given by

$$\gamma_1(i, j) = \alpha 10\log_{10} l(i, j) \text{ (dB)}, \tag{5}$$

where α is the path loss exponent. The stochastic component $\gamma_2(i, j)$ is assumed to follow log-normal probability density function. Therefore, $\gamma_2(i, j)$ in dB follows normal probability density function [20, 21], i.e.,

$$f_{\gamma_2}(\gamma_2) = \frac{1}{\sqrt{2\pi}\sigma}\exp\left(-\frac{\gamma_2^2}{2\sigma^2}\right) \text{ (dB)}. \tag{6}$$

Typically, the value of standard deviation σ ranges up to 10 dB. The total attenuation in dB is the summation of two above components, specifically

$$\gamma(i, j) = \gamma_1(i, j) + \gamma_2(i, j) \text{ (dB)}. \tag{7}$$

From the perspective of signal transmission, node j receives the signal from i properly if $p_r(j)$ is larger than or equal to a certain threshold power $p_{r,th}(j)$, which can be referred as receiver sensitivity. If $p_r(j) \geq p_{r,th}(j)$, it is said that node i can establish a wireless link to node j. We assume that channels are symmetric and all nodes, i.e. SUs and PUs, have the same p_t and $p_{r,th}$. Those assumptions will be used to analyze the connectivity of CRAHNs in the following section.

3. Connectivity analysis of CRAHNs

In this section, we analyze the connectivity of CRAHNs from the viewpoint of SU. First, we study the link connectivity and average number of neighbors of a SU in standalone secondary network without the impact of primary network. Then, we extend to the case where secondary network coexists with primary network, which is considered as the connectivity of CRAHNs with shadow fading.

3.1 Link probability between two users

For a given $p_t(i)$ and $p_{t,th}(j)$, two users i and j are considered as neighboring nodes if the signal attenuation between them satisfies

$$\gamma(i,j) \le \gamma_{th}, \tag{8}$$

where the threshold attenuation is

$$\gamma_{th} = 10\log_{10}\left(\frac{p_t(i)}{p_{r,th}(j)}\right) \text{ (dB)}. \tag{9}$$

Let denote $\Lambda(i,j)$ the event that there is a wireless link between i and j which are far way at distance $l(i,j)$. The probability of $\Lambda(i,j)$ is given by

$$P\left(\Lambda(i,j)\,|\,l(i,j)\right) = P\left(\gamma(i,j) \le \gamma_{th}\,|\,l(i,j)\right). \tag{10}$$

From (7), we have $\gamma_2(i,j) = \gamma(i,j) - \gamma_1(i,j)$. Moreover, when the distance $l(i,j)$ between them is known, the deterministic component of signal attenuation $\gamma_1(i,j)$ can be directly calculated by (5). Hence, probability of $\Lambda(i,j)$ can be calculated by taking integration with respect to $\gamma_2(i,j)$, i.e.,

$$P\left(\Lambda(i,j)\,|\,l(i,j)\right) = \int_{-\infty}^{\gamma_{th}-\gamma_1(i,j)} f_{\gamma_2}(\gamma_2)d\gamma_2. \tag{11}$$

Substituting the expressions of $\gamma_1(i,j)$ and $\gamma_2(i,j)$ in (5) and (6), respectively, into (11), we obtain

$$P\left(\Lambda(i,j)\,|\,l(i,j)\right) = \int_{-\infty}^{\gamma_{th}-\alpha 10\log_{10} l(i,j)} \frac{1}{\sqrt{2\pi}\sigma}\exp\left(-\frac{\gamma_2^2}{2\sigma^2}\right)d\gamma_2. \tag{12}$$

Solving (12) yields

$$P\left(\Lambda(i,j)\,|\,l(i,j)\right) = \frac{1}{2} - \frac{1}{2}erf\left(\frac{10\alpha}{\sqrt{2}\sigma}\log_{10}\frac{l(i,j)}{r_0}\right), \tag{13}$$

where the disk transmission range

$$r_0 = 10^{\frac{\gamma_{th}}{\alpha 10}}. \tag{14}$$

is the transmission range in the case of without shadow fading ($\sigma = 0$), and $erf(.)$ is the error function which is defined as

$$erf(x) = \frac{2}{\sqrt{\pi}}\int_0^x \exp\left(-t^2\right)dt. \tag{15}$$

The derivation of (13) from (12) is presented in detail in Appendix A.

3.2 Number of neighbors of a secondary user

From the probability of having wireless link between two users as in (13), we study the number of neighbors D of a specific secondary user. The expected value of D can be calculated by taking integration of $\rho P\left(\Lambda(i,j)\,|\,l(i,j)\right)$ over the entire network, i.e.,

$$E[D] = \rho \int_0^{2\pi} \int_0^{\infty} P(\Lambda \,|\, l) l.dl.d\phi$$

$$= 2\pi\rho \int_0^{\infty} P(\Lambda \,|\, l) l.dl\,. \tag{16}$$

In general, a closed-form expression for (16) cannot be obtained. However, it can quickly and accurately be numerically computed with the support of calculation tool such as MATLAB [22]. It should be noted that neighbors of a SU can be SUs and PUs. Thus, $E[D]$ corresponding to neighboring SUs and neighboring PUs of that SU can be obtained by replacing ρ in (16) with ρ_S and ρ_P, respectively.

3.3 Communication probability of a secondary user

We have studied the link probability between any two users, i.e. SU-SU and SU-PU, in Section 3.1. Two users that have a link between each other are called neighbors in the network topology. Based on this derivation, we now investigate the communication probability of a SU in CRAHNs under the impact of spectrum sensing efficiency of SU. The communication probability of a SU means the probability that a secondary transmitter (a secondary receiver) can communicate properly with at least one neighbor SUs while do not interfere with active primary receivers (being interfered by primary transmitters).

From the perspective of SU in CRAHNs, wireless connection of a specific SU exists if the following two conditions are fulfilled:

i) *It has at least one neighboring SU.* From (1), the probability that a SU has no neighboring node is given by

$$P_{M,SU}(0) = e^{-E_{SU}[D]}\,. \tag{17}$$

Thus, the probability that a SU has at least one neighboring SU is

$$\Phi_{com} = 1 - P_{M,SU}(0) = 1 - e^{-E_{SU}[D]}\,, \tag{18}$$

where $E_{SU}[D]$ is the expected number of SUs which are neighbors of the considered SU.

ii) *It does not interfere with or being interfered by active neighboring PUs.* According to (1), the probability that a SU has m PUs as neighbors is

$$P_{M,PU}(m) = \frac{E_{PU}[D]^m}{m!} e^{-E_{PU}[D]}, \tag{19}$$

where $E_{PU}[D]$ is the expected number of PUs which are neighbors of the examined SU. We should remind that the values of $E_{SU}[D]$ in (17) and $E_{PU}[D]$ in (19) are computed by substituting ρ in (16) with ρ_S and ρ_P, respectively.

Moreover, all of these neighboring PUs should be in inactive state with probability given by (2), that is

$$P_X(0)^m = \left(e^{-\lambda_P}\right)^m = e^{-m\lambda_P}. \tag{20}$$

Then, the probability that a SU does not interfere with or being interfered by any active neighboring PUs in the network is formulated as

$$\Theta_{com} = \sum_{m=0}^{N_P} P_{M,PU}(m) P_X(0)^m. \tag{21}$$

Finally, taking into account the primary-user detection probability P_d and false alarm probability P_f, the communication probability of a SU in CRAHNs is given by

$$\begin{aligned} P_{com} &= \Phi_{com} \cdot \left(\Theta_{com} P_d + (1-\Theta_{com}) P_f\right) \\ &= \left(1-e^{-E_{SU}[D]}\right)\left(P_d \sum_{m=0}^{N_P} \frac{E_{PU}[D]^m}{m!} e^{-E_{PU}[D]} e^{-m\lambda_P} + P_f\left(1-\sum_{m=0}^{N_P} \frac{E_{PU}[D]^m}{m!} e^{-E_{PU}[D]} e^{-m\lambda_P}\right)\right). \end{aligned} \tag{22}$$

In the case of perfect spectrum sensing, i.e. $P_d = 1$ and $P_f = 0$, the communication probability of a secondary user becomes

$$\begin{aligned} P_{com}^* &= \Phi_{com} \cdot \Theta_{com} \\ &= \left(1-e^{-E_{SU}[D]}\right)\left(\sum_{m=0}^{N_P} \frac{E_{PU}[D]^m}{m!} e^{-E_{PU}[D]} e^{-m\lambda_P}\right). \end{aligned} \tag{23}$$

3.4 Probability of direct communication between two secondary users

In CRAHNs, two secondary users can directly communicate with each other if:

i) *There are no active primary receiver and primary transmitter inside the coverage area of secondary transmitter and secondary receiver, respectively*. Since the impact of secondary transmitter on primary receiver and the impact of primary transmitter on secondary receiver are independent and have the same distribution, from (21) in Section 3.3, the probability that both secondary transmitter and secondary receiver can operate properly is

$$\Theta_{link} = \Theta_{com}^{tx} \cdot \Theta_{com}^{rx} = \left(\sum_{m=0}^{N_P} P_{M,PU}(m) P_X(0)^m\right)^2. \tag{24}$$

ii) *Under a certain shadow fading condition, there exists a wireless link between them*. The probability that there exist wireless link between two nodes under shadow fading is given in (13), Section 3.1.

Similarly, the probability of direct communication between two secondary users when primary-user detection probability P_d and false alarm probability P_f are taken into account is

$$P_{link} = P(\Lambda \mid l)\left(\Theta_{com} P_d + (1-\Theta_{com}) P_f\right)^2$$

$$= \left(\frac{1}{2} - \frac{1}{2} erf\left(\frac{10\alpha}{\sqrt{2}\sigma} \log_{10} \frac{l(i,j)}{r_0} \right) \right) \times$$

$$\left(P_d \sum_{m=0}^{N_P} \frac{E_{PU}[D]^m}{m!} e^{-E_{PU}[D]} e^{-m\lambda_P} + P_f \left(1 - \sum_{m=0}^{N_P} \frac{E_{PU}[D]^m}{m!} e^{-E_{PU}[D]} e^{-m\lambda_P} \right) \right)^2 . \quad (25)$$

In the case of perfect spectrum sensing, probability of direct communication between two secondary user becomes

$$P_{link}^* = P(\Lambda \mid l)\left(\Theta_{com}\right)^2$$

$$= \left(\frac{1}{2} - \frac{1}{2} erf\left(\frac{10\alpha}{\sqrt{2}\sigma} \log_{10} \frac{l(i,j)}{r_0} \right) \right) \left(\sum_{m=0}^{N_P} \frac{E_{PU}[D]^m}{m!} e^{-E_{PU}[D]} e^{-m\lambda_P} \right)^2 . \quad (26)$$

4. Numerical results and discussions

In this section, we present numerical results of the effect of shadow fading on the connectivity of CRAHNs. We verify the analytical results by comparing them with simulation results. In the simulation, SUs and PUs are distributed according to a homogeneous Poisson process with density of ρ_S and ρ_P, respectively. We conduct simulation by using MATLAB on a computer workstation equipped with 3.5 GHz (Intel Core i7-3570 Quad) processor, 4 GB of RAM, and Windows 7. In all demonstrated network topologies used in this section, red nodes denote PUs, blue node denotes source SU, green node denotes destination SU, white nodes denote intermediate SUs, blue solid lines denote communication links between two SUs, and dashed red lines denote communication links between PU and SU. The simulation results is calculated by averaging 50000 Monte Carlo simulation network topologies. For each network topology, a new random node's location is used. Simulation time varies from 0.4 hour to 1.7 hours, depending on the values of network parameters used in the simulation.

Fig. 3 illustrates the difference in communication possibility of a SU in non fading and shadow fading environment. Specifically, **Fig. 3(a)** and **Fig. 3(b)** depict the cases where SU is not affected by any active PUs. For non fading situation as in **Fig. 3(a)**, a SU only has wireless connection with other SUs staying inside its circular transmission area. However, for shadowing fading condition as in **Fig. 3(b)**, a SU may have wireless link with other SUs staying outside its transmission area in **Fig. 3(a)**. The wireless link establishment between active PUs and SUs also has the same behavior, which results in different communication probability of a specific SU. For example, with the same distance between an active PU and a SU, this SU is allowed to communicate with other SUs inside its transmission area as in **Fig. 3(c)**, i.e. the case of non fading, because the distance from it to an active PU is larger than transmission range. Meanwhile, in **Fig. 3(d)**, due to the effect of shadow fading, the wireless link between an active PU and a SU is possible. Thus, this SU is not allowed to communicate with other SUs. In the reverse scenario, if the distance between an active PU and a SU is smaller than transmission range, this SU is not allowed to communicate with other SUs inside its transmission area as in **Fig. 3(e)**, i.e. the case of non fading. Nevertheless, this situation may not happen in **Fig. 3(f)**, i.e. the case of shadowing fading. Athough the distance between an active PU and a SU is the same as in **Fig. 3(e)**, the wireless link between PU and SU does not exist due to the effect of shadow fading. Consequently, the SU is allowed to communicate with

other SUs.

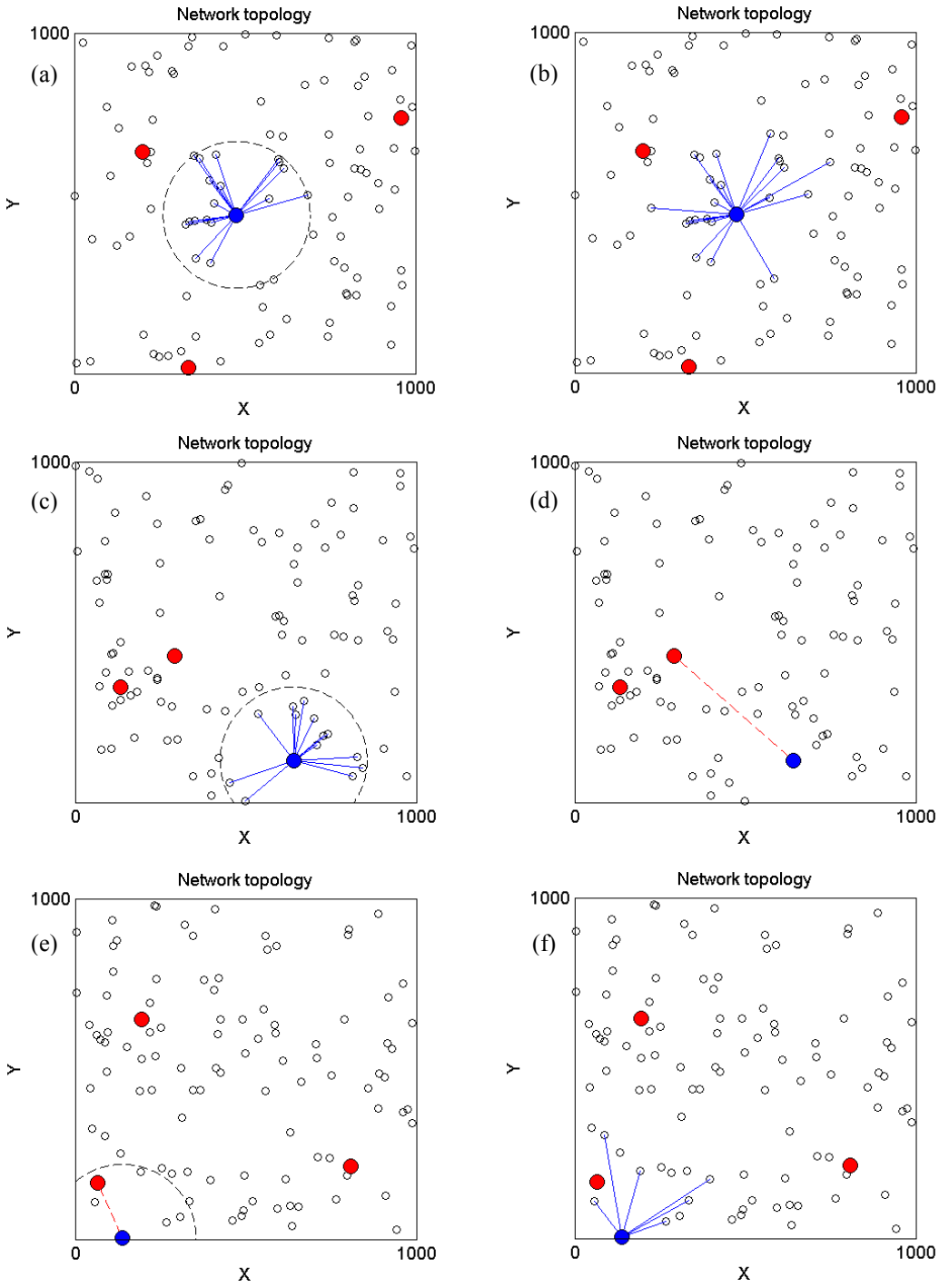

Fig. 3. Illustration of communication possibility of a SU in CRAHNs in non fading ($\sigma = 0$) and shadow fading ($\sigma = 4$) environment; $N_S = 100$, $N_P = 10$, $\lambda_P = 0.3$, $\alpha = 3$, $\gamma_{th} = 70$ dB

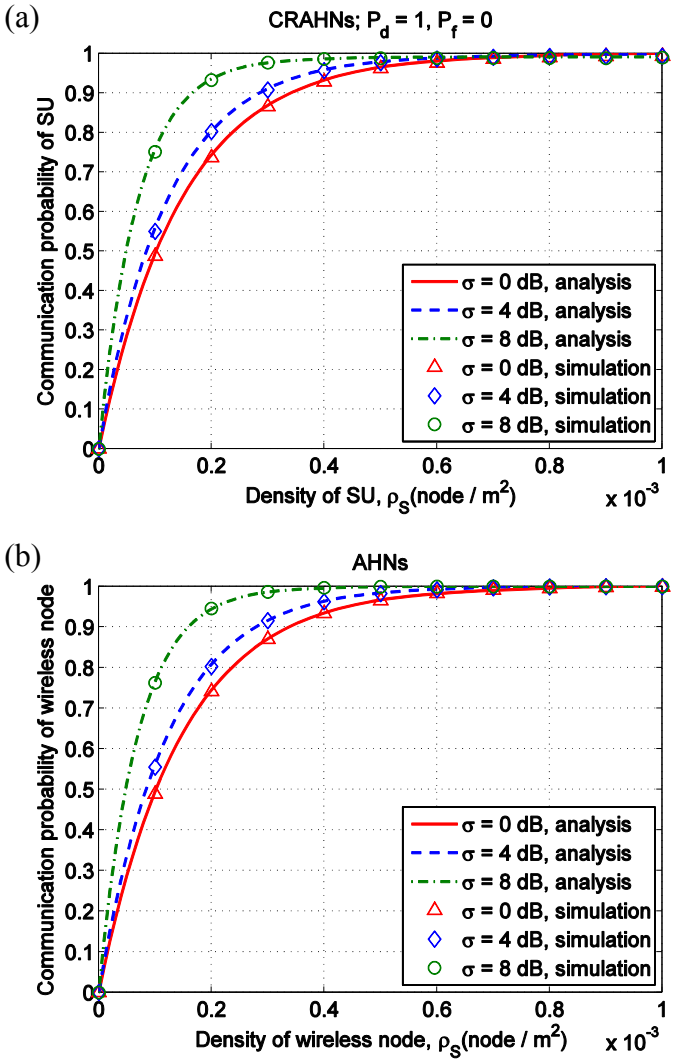

Fig. 4. Comparison of the communication probability of SU in CRAHNs in the case of perfect spectrum sensing and of wireless node in AHNs versus node (SU)'s density for different shadow fading conditions; $\rho_P = 3\times10^{-6}$ nodes/m^2, $\lambda_P = 0.3$, $\alpha = 3$, $\gamma_{th} = 50$ dB

Fig. 4(a) shows the communication probability of SU in CRAHNs in the case of perfect spectrum sensing ($P_d = 1$, $P_f = 0$) of SU versus SU's density for different shadow fading degree. For comparison, the communication probability of AHNs versus node's density in the same fading conditions is presented in **Fig. 4(b)**. The communication probability of a SU in CRAHNs means the probability that a SU has at least one neighboring SU and available spectrum band to communicate with these neighboring SUs. From **Fig. 4(a)**, we can see that higher SU's density and higher shadow fading degree increase the communication probability of SU in CRAHNs. Particularly, as density of SU ρ_S increases, communication probability of SU increases sharply in shadow fading environment with $\sigma = 8$ dB, reaching stable value of around 0.98 at $\rho_S = 0.4\times10^{-3}$ node/m^2. Meanwhile, communication probability of SU reaches stable value at $\rho_S = 0.6\times10^{-3}$ node/m^2 in the shadow fading environment with $\sigma = 4$ dB. In non shadowing environment, i.e. $\sigma = 0$ dB, communication probability of SU requires higher

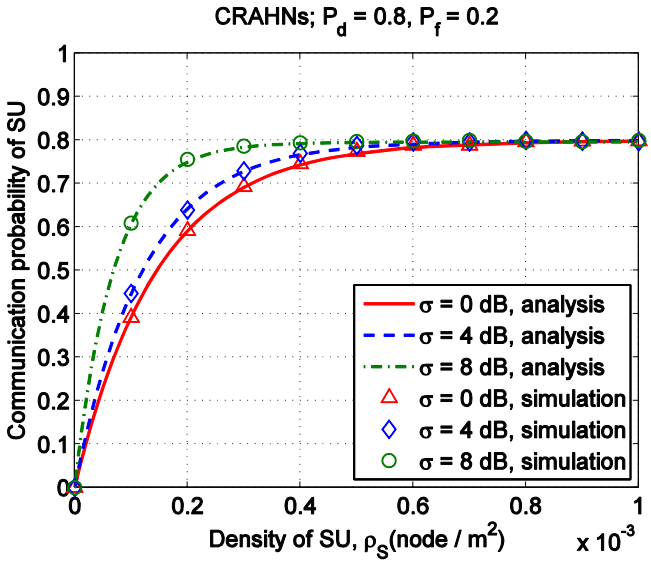

Fig. 5. Communication probability of SU versus SU's density in the case of imperfect spectrum sensing of SU ($P_d = 0.8$, $P_f = 0.2$) for different shadow fading conditions

SU's density, $\rho_S = 0.7\times10^{-3}$ node/m^2, to reach stable value. The same behavior of commnication probability can be observed in **Fig. 4(b)** for the case of AHNs, except that the commnication probability of wireless node reaches stable value faster especially when $\sigma = 8$ dB. It is because wireless nodes have more opportunity to communicate with each other when there are no PUs in the network. For other conditions, i.e. $\sigma = 4$ dB and $\sigma = 0$ dB (non fading), the values of commnication probability in AHNs and CRAHNs are insignificantly different. It may because the PU's density, $\rho_P = 3\times10^{-6}$ node/m^2, used in the simulation of CRAHNs is not very high.

In constrast to **Fig. 4(a)**, **Fig. 5** depicts the communication probability of SU in CRAHNs in the case of imperfect spectrum sensing ($P_d = 0.8$, $P_f = 0.1$) of SU versus SU's density for different shadow fading degree. As can be seen in **Fig. 5**, the spectrum sensing efficiency of SU greatly influences its communication probability. Particularly, the maximum communication probability of SU in **Fig. 5** is much lower than that in **Fig. 4(a)**. An important feature which can be seen in **Fig. 5** is that when the influence of PU is small (i.e. Θ_{com} in (22) goes to 1), the communication probability of SU is $P_{com} \approx \Phi_{com}\cdot P_d$. In other words, the correct primary-user dectection efficiency of SU directly relates to its achievable maximum communication probability. This observation is confirmed by simulation results in **Fig. 5**.

Fig. 6 shows the comparison of the connection probability of a SU in CRAHNs versus the average active rate of PU for different shadow fading conditions and primary-user detection ability of SU. As observed from both **Fig. 6(a)** and **Fig. 6(b)**, the impact of shadow fading degree on connection probability of a SU in CRAHNs dominates that of the average active rate of PU. In particular, increasing the average active rate of PU does not reduce much the wireless connection probability compared with reducing SU's density. However, high fading variance σ greatly 'helps' to improve the communication probability of a SU. This surprising effect can be explained as follows: For a given SU, shadow fading may take away wireless links to other SUs that locate within a distance r_0 from the considered SU, but in turn, it adds wireless links to nodes that locate further away. On average, the number of added links is

higher than the number of removed links because the number of potential neighboring SUs of a given SU is exponentially proportional to the distance, i.e. $l(i, j)$, from them to that SU. Another observation from **Fig. 6(b)** is that the imperfect primary-user detection ability of SU, together with higher active rate of PU, reduces its communications probability in the same network conditions used in **Fig. 6(a)**. The slight difference between simulation results and analysis results can be explained as follows. Similar to all previous works in the literature, for simplicity of theoretical expressions, all wireless nodes are assumed to be placed in infinite network area. Thus, the *effective coverage areas* of wireless nodes are always circular. However, to model real network circumstance, we simulate with finite network area. Consequently, wireless nodes which are near the edge of network area do not have perfect circular coverage area. This fact is called *border effect*, which already discussed in [23]. The border effect is alleviated as the network area and node density increase.

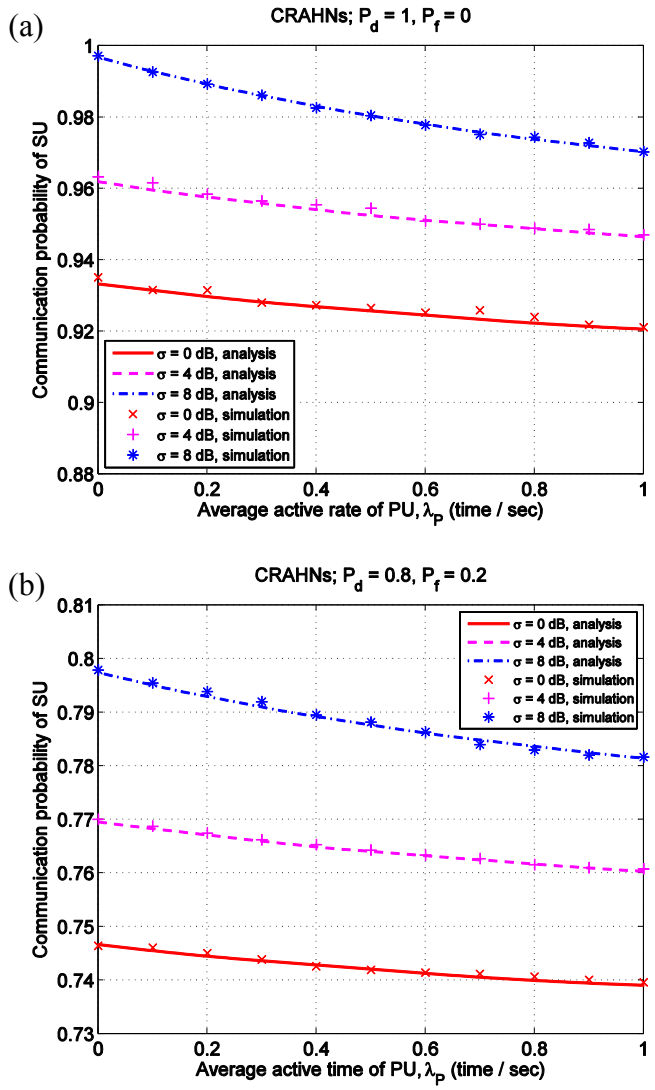

Fig. 6. Comparison of the communication probability of SU versus PU's average active rate in the case of (a) perfect spectrum sensing and (b) imperfect spectrum sensing of SU for different shadow fading conditions; $\rho_S = 4\times10^{-3}$ node/m^2 , $\rho_P = 3\times10^{-6}$ node/m^2, $\alpha = 3$, $\gamma_{th} = 50$ dB

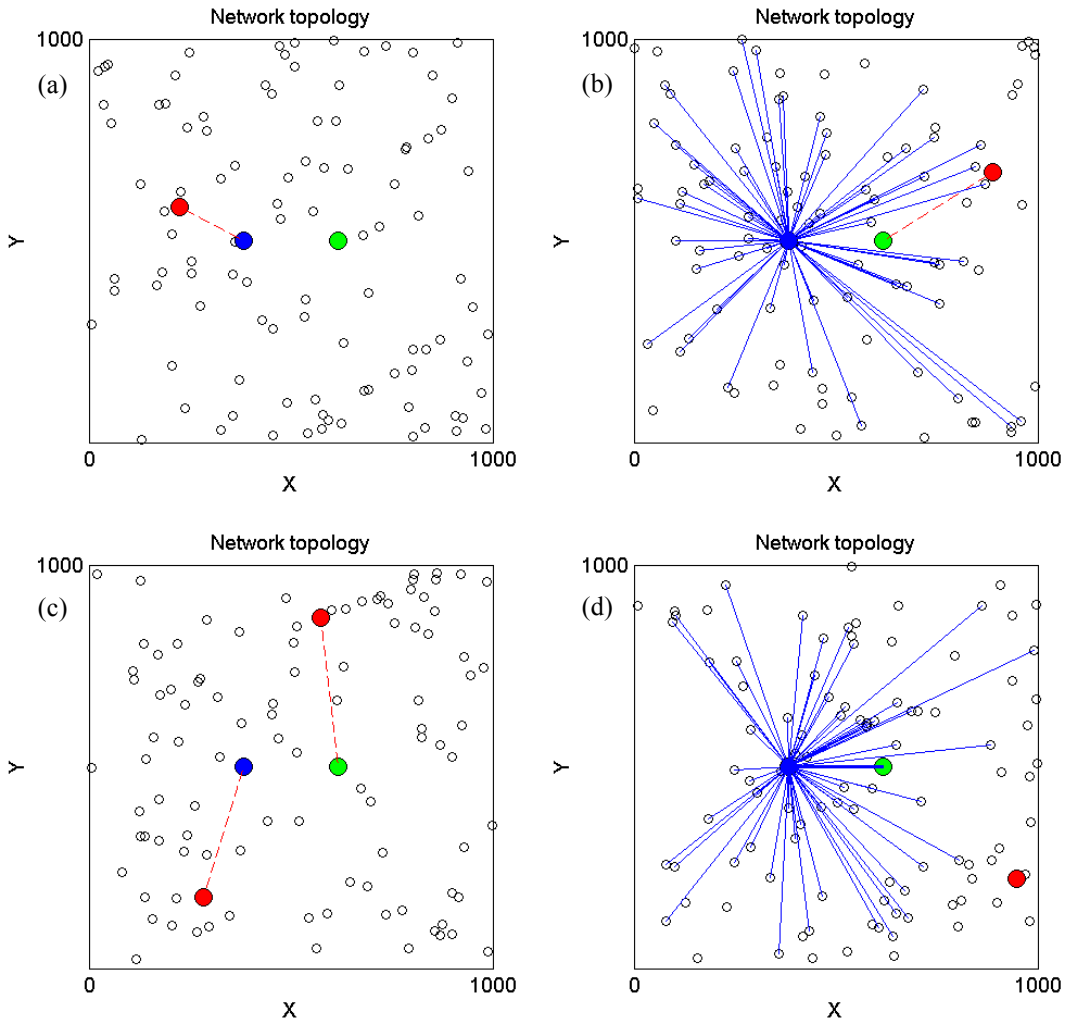

Fig. 7. Illustration of direct communication possibility between two SUs in CRAHNs with shadow fading environment; $\rho_S = 1\times10^{-4}$ node/m^2 , $\rho_P = 1\times10^{-5}$ node/m^2, $\lambda_P = 0.1$, $\alpha = 3$, $\sigma = 4$ dB, $\gamma_{th} = 80$ dB

Next, we will study the possibility of having direct communication link between two SUs locating at a relative distance l in CRAHNs with shadow fading environment. **Fig. 7** consists of several network topologies to illustrate the direct communication possibility between two SUs in CRAHNs in shadow fading environment. As we know, two SUs can communicate directly if: (i) none of them is affected by any active PUs and (ii) they can establish a direct communication link between them. **Fig. 7(a)**, **Fig. 7(b)**, and **Fig. 7(c)** depict the cases where two SUs cannot communicate directly because secondary transmitter, secondary receiver, and both secondary transmitter and secondary receiver do not allowed to work properly. **Fig. 7(d)** presents the case where two SUs can sucessfully establish direct communication link (represented as bold blue line) between them due to these SUs are not affected by any active PUs and the power attenuation between them is less than the threshold $\gamma_{th} = 80$ dB.

Fig. 8 shows the probability of having wireless link between two nodes (SUs) versus l/r_0 for $\alpha = 2$ and $\alpha = 3$ with different values of shadow fading degree σ and primary-user detecting ability of SU. As observed from **Fig. 8**, the relative distance between two users as well as

fading degree have significant impact on the possibility of being neighbors of two users in both CRAHNs and AHNs. Particularly, when the distance between two SUs is smaller than the

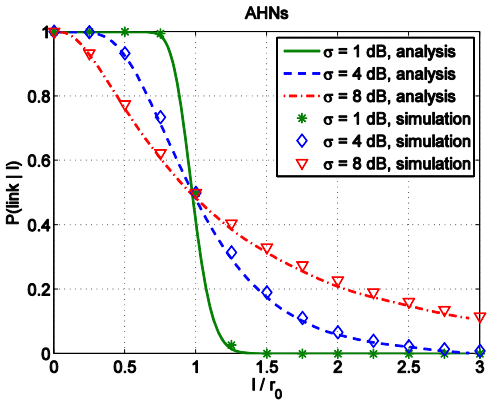

(a) Path loss exponent $\alpha = 2$, AHNs

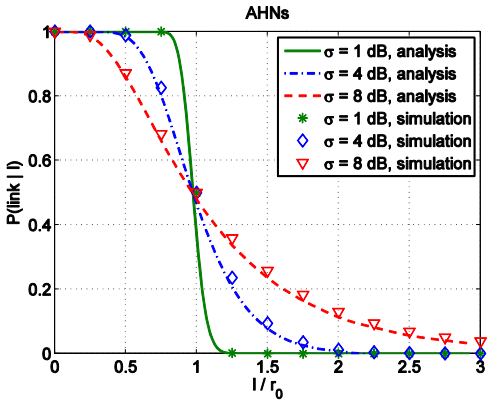

(b) Path loss exponent $\alpha = 3$, AHNs

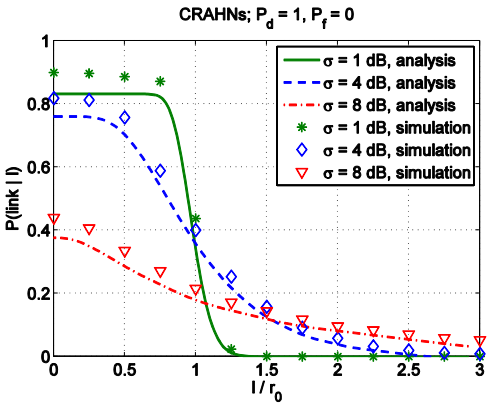

(c) $\alpha = 2$, CRAHNs, $P_d = 1$, $P_f = 0$

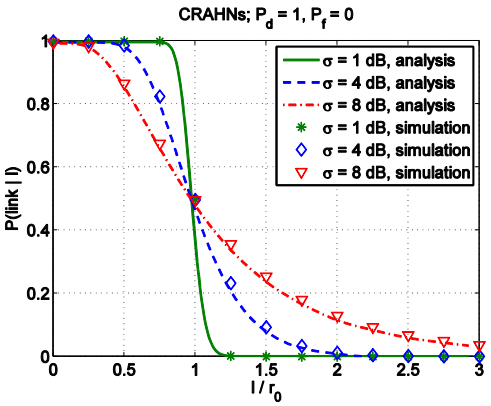

(d) $\alpha = 3$, CRAHNs, $P_d = 1$, $P_f = 0$

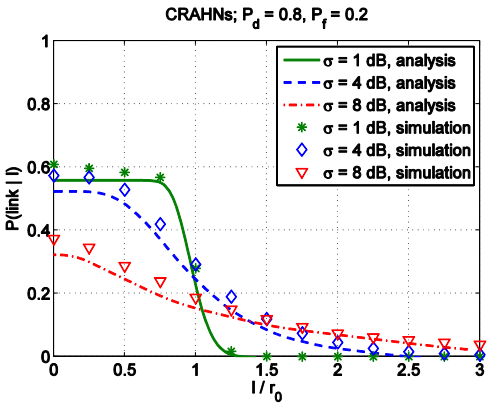

(e) $\alpha = 2$, CRAHNs, $P_d = 0.8$, $P_f = 0.2$

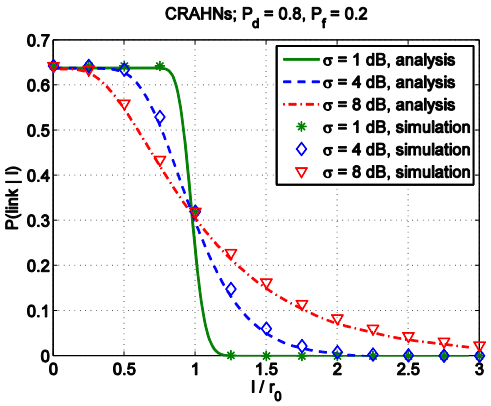

(f) $\alpha = 3$, CRAHNs, $P_d = 0.8$, $P_f = 0.2$

Fig. 8. Comparison of the probability that two SUs can establish a direct communication link vesus the relative distance between them for different fading conditions and spectrum sensing efficiency of SU and that in AHNs; $\rho_S = 1\times10^{-4}$ node/m^2 , $\rho_P = 3\times10^{-6}$ node/m^2, $\lambda_P = 0.1$, $\gamma_{th} = 50$ dB

disk transmission range r_0 correlating with the deterministic component of signal attenuation, two SUs have significantly high possibility to communicate directly. In AHNs, as the distance between two nodes increases, the probability that they can establish a direct communication link remarkably reduces. In addition, the reducing rate of direct communication probability of two nodes depends on the path loss exponent α. The lower α is, the lower reducing rate of direct communication probability is. It is because path loss exponent α affects the disk transmission range r_0 as given by (14). For example, as shown in **Fig. 8(a)** and **Fig. 8(b)**, with γ_{th} = 50 dB considered in this analyzing scenario, α = 2 corresponding to r_0 = 316.228 m provides lower reducing rate of direct communication probability of two nodes than when α = 3 corresponding to r_0 = 46.416 m. In CRAHNs, in the case of perfect spectrum sensing of SU (P_d = 1, P_f = 0), the pattern of direct communication probability of two SUs when α = 3 (refer to **Fig. 8(d)**) is quite similar to that of AHNs. However, when α = 2 (refer to **Fig. 8(c)**), the pattern of direct communication probability of two SUs is significantly different from that of AHNs. More specifically, when l/r_0 decreases, the maximum value of direct communication probability of two SUs in CRAHNs is noticeably lower compared with AHNs. It is due to the fact that lower path loss exponent α results in larger disk transmission range r_0, which increases the possibility of having active PUs interfere with communication of SUs.

The effect of imperfect spectrum sensing of SU on the probability of direct communication between two SU is also studied and the results are plotted in **Fig. 8(e)** and **Fig. 8(f)**. We can see that the patterns of **Fig. 8(e)** and **Fig. 8(f)** are similar to those in **Fig. 8(a)** and **Fig. 8(d)**, except that the maximum achievable link probability is remarkably lower. This is because the decrease in primary-user dectection ability of SU reduces the communication possiblility of both secondary transmitter and secondary receiver and thus, results in much lower maximum achievable direct communication probability.

In general, the simulation results in **Fig. 8** are in good agreement with the analytical results. Only when path loss exponent α is small (α = 2 in this case) and the distance between secondary transmitter and secondary receiver is less than the disk transmission range, there is a gap between the simulation results and analysis results. The explanations for this observation are follows. According to (16), to obtain analytical result of expected number of neighbors (SUs and PUs) of a SU, we take integration of $P(\Lambda(i, j)|l(i, j))$ with respect to $l(i, j)$ over the infinite network area, i.e. the values of $l(i, j)$ are from 0 to infinite. In addition, $P(\Lambda(i, j)|l(i, j))$ itself is a function of α. Thus, when path loss exponent α is small and the distance $l(i, j)$ between transmitter i and receiver j goes to 0, the impact of boundary effect on the gap between simulation results and analysis results is exponentially higher because in simulation scenarios the possible values of $l(i, j)$ are only from 0 to a finite number. This gap is reduced when the border effect is mitigated.

We are now interested in investigating the communication probability of two arbitrary SUs in CRAHNs with shadow fading environment. It is noted that the communication of two arbitrary SUs includes both direct communication and indirect communication, i.e. communication through several intermediate SUs on multi-hop path.

Fig. 9(a) and **Fig. 9(b)** present the cases where source SU (green node) cannot communicate with destination SU (blue node) because destination node or both source node and destination node are affected by active PUs, respectively. In **Fig. 9(c)** and **Fig. 9(d)**, source SU and destination SU are not affected by any active PUs. There exist multi-hop paths between source SU and destination SU in **Fig. 9(c)**. However, there are no paths between these two nodes in **Fig. 9(d)**.

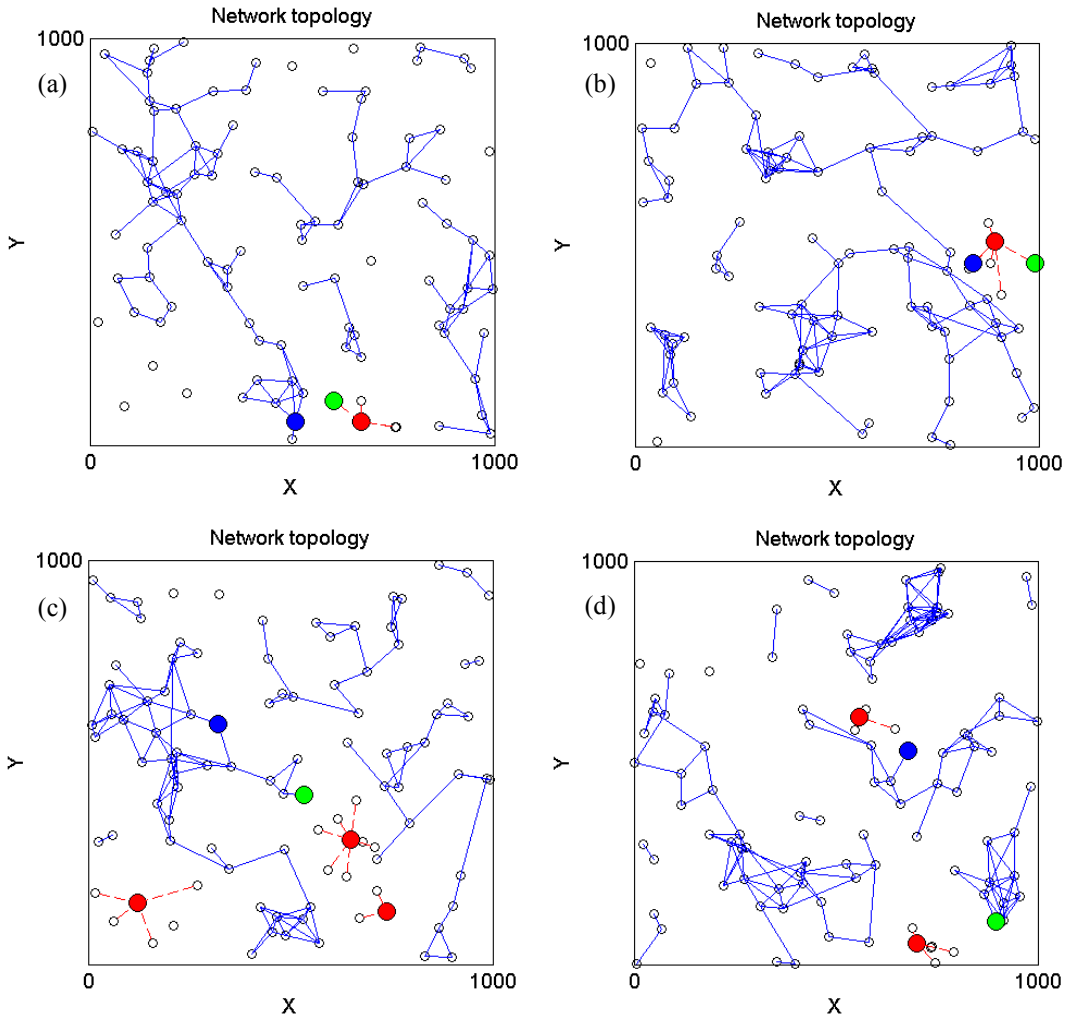

Fig. 9. Illustration of multi-hop communication possibility between two SUs in CRAHNs with shadow fading environment; $\rho_S = 1\times10^{-4}$ node/m^2 , $\rho_P = 1\times10^{-5}$ node/m^2, $\lambda_P = 0.3$, $\alpha = 3$, $\sigma = 4$ dB, $\gamma_{th} = 60$ dB

Fig. 10 shows the comparison of the communication probability of a SU and multi-hop path connectivity between two arbitrary SUs in CRAHNs versus SU's density for different fading conditions and spectrum sensing efficiency. As we can see in **Fig. 10**, in the same fading condition, multi-hop path connectivity is significantly lower than the communication probability of a SU. It is because the connectivity of multi-hop path not only closely depends on the communication probability of a SU but also depends on the path length in terms of hop count. With the same communication probability of a SU, the longer that path is, the lower possibility that source node and destination node can be connected. As shown in **Fig. 10(b)**, the decrease in spectrum sensing efficiency greatly reduces the communication probability of a SU and multi-hop path connectivity between two arbitrary SUs compared with those in **Fig. 10(a)**.

Fig. 11 shows the multi-hop connectivity of two arbitrary SUs in CRAHNs versus SU's density for different fading conditions and spectrum sensing efficiency. From **Fig. 11**, we can observe some interesting features as follows. When γ_{th} = 50 dB, the higher shadow

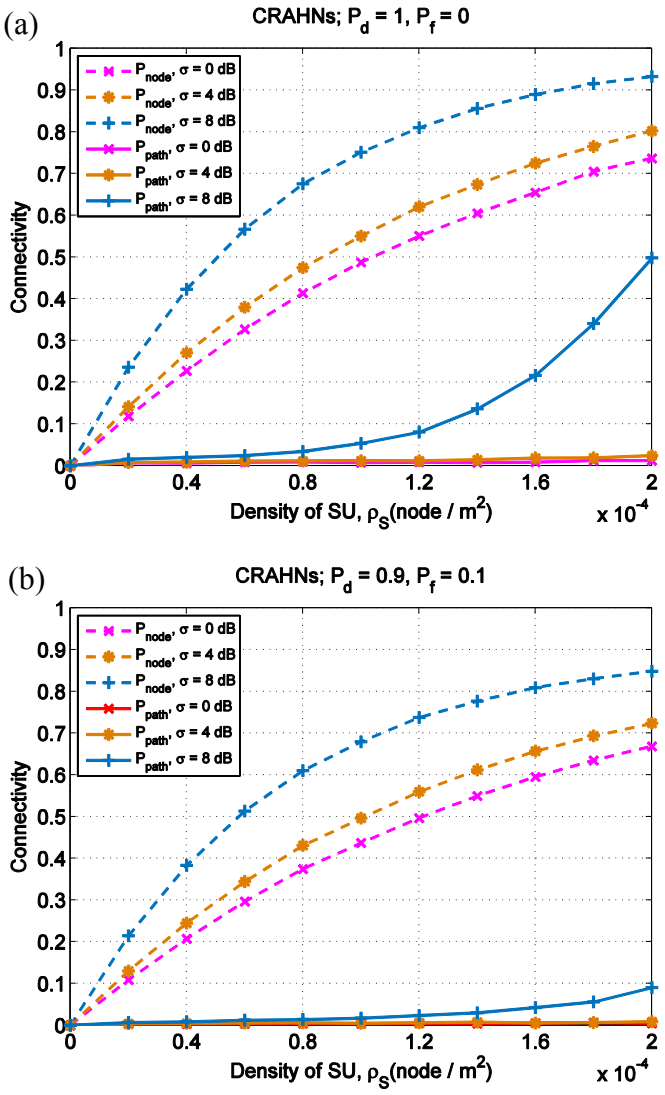

Fig. 10. Comparison of the communication probability of a SU and multi-hop path connectivity between two arbitrary SUs in CRAHNs versus density of SU with different fading conditions; $\rho_P = 3\times10^{-6}$ node/m^2, $\lambda_P = 0.3$, $\alpha = 3$, $\gamma_{th} = 50$ dB

fading degree, i.e. higher value of σ, provides higher multi-hop connectivity as can also be seen in **Fig. 10**. However, when γ_{th} is increased to 65 dB, the same behavior does not happen. It is because the disk transmission range r_0 corresponding to the deterministic component of signal attenuation depends on the value of signal attenuation threshold as expressed in (14). The values of r_0 are 46.416 m and 146.780 m when $\alpha = 3$, $\gamma_{th} = 50$ dB and 65 dB, respectively. The significant increase in disk transmission range r_0 together with high shadow fading degree results in more possibility that SU will be interfered by active PUs. Consequently, the stable value of multi-hop connectivity in the case of higher shadow fading degree is smaller than that in the case of lower shadow fading degree. We can also see that in the same network conditions, the multi-hop connectivity in **Fig. 11(b)** is much lower than that in **Fig. 11(a)** due to the degrading spectrum sensing efficiency of SU.

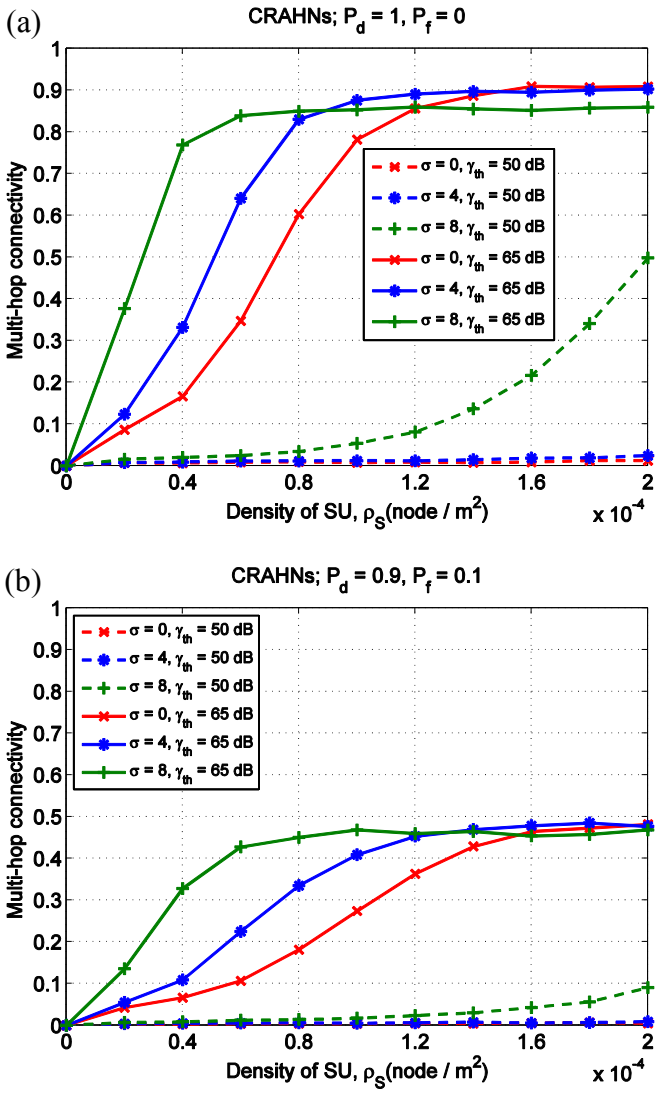

Fig. 11. Multi-hop connectivity of two arbitrary SUs in CRAHNs versus density of SU for different fading conditions and spectrum sensing efficiency; $\rho_P = 3\times10^{-6}$ node/m^2, $\lambda_P = 0.3$, $\alpha = 3$

5. Conclusion

We have studied the connectivity of CRAHNs in shadow fading environment. As opposed to previous research works on the connectivity of CRAHNs in the literature, we take into account the stochastic shadowing effects between two users. The investigation into the connectivity of CRAHNs in fading environment is exhaustively conducted in three aspects: communication probability of a SU, direct communication link probability, and multi-hop path connectivity of two SUs. Using both analytical and simulation methods, we observe several interesting characteristics of the impact of shadowing and PU's existence on the connectivity of CRAHNs: (i) for a given value of path loss exponent α, a higher fading variance σ improves the connectivity, (ii) the average active rate of PU does not have noticeable impact on the connectivity compared to that of SU density and shadow fading degree, (iii) the multi-hop

connection probability of two arbitrary SUs is significantly lower than communication probability of a SU with the same network condition, and the stable value of multi-hop connectivity in the case of higher shadow fading degree is smaller than that in the case of lower shadow fading degree, and (iv) the spectrum sensing efficiency of SU greatly affects the connectivity of secondary network. The analysis in this paper can be used as a framework when considering the connectivity of CRAHNs with other kinds of fading effects. Moreover, the results in this paper can be combined with the results of connectivity dynamics, e.g. the stochastic properties of path duration between two nodes [24-25] in the literature, for designing and evaluating more practical CRAHNs.

Appendix A: Derivation of (13)

Starting from (12), i.e., $P\left(\Lambda(i,j)\,|\,l(i,j)\right)=\int_{-\infty}^{\gamma_{th}-\alpha 10\log_{10} l(i,j)}\frac{1}{\sqrt{2\pi}\sigma}\exp\left(-\frac{\gamma_2^2}{2\sigma^2}\right)d\gamma_2$. Let us denote $t=\frac{\gamma_2}{\sqrt{2}\sigma}$, hence $\gamma_2=\sqrt{2}\sigma t$ and $d\gamma_2=\sqrt{2}\sigma dt$. When $\gamma_2=-\infty$, $t=-\infty$; and when $\gamma_2=\gamma_{th}-\alpha 10\log_{10} l(i,j)$, $t=t_0=\frac{\gamma_{th}-\alpha 10\log_{10} l(i,j)}{\sqrt{2}\sigma}$.

Therefore, (12) becomes

$$P\left(\Lambda(i,j)\,|\,l(i,j)\right)=\int_{-\infty}^{t_0}\frac{1}{\sqrt{\pi}}\exp\left(-t^2\right)dt \tag{27}$$

$$=\int_{-\infty}^{0}\frac{1}{\sqrt{\pi}}\exp\left(-t^2\right)dt+\int_{0}^{t_0}\frac{1}{\sqrt{\pi}}\exp\left(-t^2\right)dt. \tag{28}$$

Since $erf(x)=\frac{2}{\sqrt{\pi}}\int_0^x\exp\left(-t^2\right)dt$, (28) can be expressed as

$$P\left(\Lambda(i,j)\,|\,l(i,j)\right)=-\frac{1}{2}erf(-\infty)+\frac{1}{2}erf(t_0). \tag{29}$$

It should be noted that $erf(-\infty)=-1$. Then,

$$P\left(\Lambda(i,j)\,|\,l(i,j)\right)=\frac{1}{2}+\frac{1}{2}erf\left(\frac{\gamma_{th}-\alpha 10\log_{10} l(i,j)}{\sqrt{2}\sigma}\right) \tag{30}$$

$$=\frac{1}{2}-\frac{1}{2}erf\left[\frac{10\alpha}{\sqrt{2}\sigma}\left(\log_{10} l(i,j)-\frac{\gamma_{th}}{10\alpha}\right)\right] \tag{31}$$

$$=\frac{1}{2}-\frac{1}{2}erf\left[\frac{10\alpha}{\sqrt{2}\sigma}\left(\log_{10} l(i,j)-\log_{10}10^{\frac{\gamma_{th}}{10\alpha}}\right)\right]. \tag{32}$$

Let us denote $r_0=10^{\frac{\gamma_{th}}{10\alpha}}$, (32) becomes

$$P\left(\Lambda(i,j)\,|\,l(i,j)\right)=\frac{1}{2}-\frac{1}{2}erf\left(\frac{10\alpha}{\sqrt{2}\sigma}\log_{10}\frac{l(i,j)}{r_0}\right). \quad (33)$$

References

[1] FCC, "Spectrum policy task force," *Technical Report*, November 2002. Article (CrossRef Link).

[2] I. F. Akyildiz, W. Y. Lee, and K. R. Chowdhury, "CRAHNs: Cognitive radio ad hoc networks," *Ad Hoc Networks*, vol. 7, no. 5, pp. 810-836, July 2009. Article (CrossRef Link).

[3] S. N. Chiu, D. Stoyan, W. S. Kendall, and J. Mecke, *Stochastic Geometry and Its Application*, 3rd Ed., Wiley, September 2013. Article (CrossRef Link).

[4] R. Meester and R. Roy, *Continuum Percolation*, 1st Ed., Cambridge University Press, May 2008. Article (CrossRef Link).

[5] K. R. Chowdhury and M. D. Felice, "Search: A routing protocol for mobile cogntive radio ad-hoc networks," *Computer Communications*, vol. 32, no. 18, pp. 1983-1997, December 2009. Article (CrossRef Link).

[6] A. S. Cacciapuoti, M. Callefi, and L. Paura, "Reactive routing for mobile cognitive radio ad hoc networks," *Ad Hoc Networks*, vol. 10, no. 5, pp. 803-815, July 2012. Article (CrossRef Link).

[7] C. Bettstetter, "On the Connectivity of Ad Hoc Networks," *The Computer Journal*, vol. 47, no. 4, pp. 432-447, 2004. Article (CrossRef Link).

[8] A. Ghosh and S. K. Das, "Coverage and connectivity issues in wireless sensor networks: A survey," *Pervasive and Mobile Computing*, vol. 4, no. 3, pp. 303-334, June 2008. Article (CrossRef Link).

[9] A. Abbagnale and F. Cuomo, "Leveraging the Algebraic Connectivity of a Cogntive Network for Routing Design," *IEEE Transactions on Mobile Computing*, vol. 11, no. 7, pp. 1163-1178, July 2012. Article (CrossRef Link).

[10] W. Ren, Q. Zhao, and A. Swami, "Connectivity of Heterogeneous Wireless Networks," *IEEE Transactions on Information Theory*, vol. 57, no. 7, pp. 4315-4332, July 2011. Article (CrossRef Link).

[11] D. Lu, X. Huang, P. Liu, and J. Fan, "Connectivity of Large-Scale Cognitive Radio Ad Hoc Networks," in *Proc. of 2012 IEEE INFOCOM*, pp. 1260-1268, March 2012. Article (CrossRef Link).

[12] J. Liu, Q. Zhang, Y. Zhang, Z. Wei, and S. Ma, "Connectivity of Two Nodes in Cognitive Radio Ad Hoc Networks," in *Proc. of 2013 IEEE Wireless Communications and Networking Conference (WCNC)*, pp. 1186-1191, April 2013. Article (CrossRef Link).

[13] D. Liu, E. Liu, Z. Zhang, R. Wang, Y. Ren, Y. Liu, I. W-H. Ho, X. Yin, and F. Liu, "Secondary Network Connectivity of Ad Hoc Cognitive Radio Networks," *IEEE Communications Letters*, vol. 18, no. 12, pp. 2177-2180, December 2014. Article (CrossRef Link).

[14] C. Bettstetter and C. Hartmann, "Connectivity of Wireless Multihop Networks in a Shadow Fading Environment," *Wireless Networks*, vol. 11, no. 5, pp. 571-579, September 2005. Article (CrossRef Link).

[15] X. Zhou, S. Durrani, and H. M. Jones, "Connectivity of Ad Hoc Networks: Is Fading Good or Bad," in *Proc. of ICSPCS 2008*, pp. 1-5, December 2008. Article (CrossRef Link).

[16] B. Xu and Q. Zhu, "Analysis of connectivity in Ad Hoc network with Nakagami-*m* fading," in *Proc. of 2014 International Conference on Information Science, Electronics and Electrical Engineering (ISEEE)*, pp. 1609-1612, April 2014. Article (CrossRef Link).

[17] D. Zhai, M. Sheng, X. Wang and Y. Zhang, "Local Connectivity of Cognitive Radio Ad Hoc Networks", in *Proc. of GLOBECOM'14*, pp. 1078-1083, December 2014. Article (CrossRef Link).

[18] D. Liu, E. Liu, Y. Ren, Z. Zhang, R. Wang and F. Liu, "Bounds on Secondary User Connectivity in Cognitive Radio Networks," *IEEE Communications Letters*, vol 19, no. 4, pp. 617-620, April 2015. Article (CrossRef Link).

[19] F. Baccelli and B. Blaszczyszyn, *Stochastic Geometry and Wireless Networks: Volume 1: Theory*, Now Publishers Inc., 2010. Article (CrossRef Link).

[20] T. S. Rappaport, *Wireless Communication: Principles and Practice*, 2nd Ed., Prentice Hall, January 2002. Article (CrossRef Link).
[21] H. N. Koivo, M. Emusrati, *Systems Engineering in Wireless Communications*, John Wiley & Sons, 2009. Article (CrossRef Link).
[22] D. Xue and Y. Chen, *Solving Applied Mathematical Problems with MATLAB*, CRC Press, 2009. Article (CrossRef Link).
[23] C. Bettstetter, "On the Minimum Node Degree and Connectivity of a Wireless Multihop Network," in *Proc. of 3rd ACM International Symposium on Mobile Ad Hoc Networking and Computing (MobiHoc '02)*, pp. 80-91, June 2002. Article (CrossRef Link).
[24] Yueh-Ting Wu, Wanjiun Liao, Chen-Lin Tsao, and Tsung-Nam Lin, "Impact of node mobility on link duration in multihop mobile networks," *IEEE Transactions on Vehicular Technology*, vol. 58, no. 5, pp. 2435-2442, June 2009. Article (CrossRef Link).
[25] L. T. Dung and B. An, "A modeling framework for supporting and evaluating performance of multi-hop paths in mobile ad-hoc wireless networks," *Computers and Mathematics with Applications*, vol. 64, no. 5, pp. 1197-1205, September 2012. Article (CrossRef Link).

Le The Dung received the B.S. degree in Electronics and Telecommunication Engineering from Ho Chi Minh City University of Technology, Vietnam, in 2008 and the M.S. degree in Electronics and Computer Engineering from Hongik University, Korea, in 2012. From 2007-2010, he joined Signet Design Solutions Vietnam as hardware designer. He is currently working toward the Ph.D. degree in Electronics and Computer Engineering with Hongik University, Korea. His major interests are routing protocols, network coding, network stability analysis and optimization in mobile ad-hoc networks and cognitive radio ad-hoc networks. He is a student member of the IEEE and the IEIE.

Beongku An received the M.S. degree in Electrical Engineering from the New York University (Polytechnic), NY, USA, in 1996 and Ph.D. degree from New Jersey Institute of Technology (NJIT), NJ, USA, in 2002, respectively. After graduation, he joined the Faculty of the Department of Computer and Information Communications Engineering, Hongik University in Korea, where he is currently a Professor. From 1989 to 1993, he was a senior researcher in RIST, Pohang, Korea. He also was lecturer and RA in NJIT from1997 to 2002. He was a president of IEIE Computer Society (The Institute of Electronics and Information Engineers, Computer Society) in 2012. From 2013, he also works as a General Chair in the International Conference, ICGHIT (International Conference on Green and Human Information Technology). His current research interests include mobile wireless networks and communications such as ad-hoc networks, sensor networks, wireless internet, cognitive radio networks, ubiquitous networks, and cellular networks. In particular, he is interested in cooperative routing, multicast routing, energy harvesting, physical layer security, visible light communication (VLC), and cross-layer technologies. Professor An was listed in Marquis Who's Who in Science and Engineering in 2006-2011, and Marquis Who's Who in the World in 2007-2014, respectively.